Molecular Biology of the Cell
Vol. 21, 2869–2879, August 15, 2010

Overlapping Roles of *Drosophila* Drak and Rok Kinases in Epithelial Tissue Morphogenesis

Dagmar Neubueser* and David R. Hipfner*†‡

*Institut de recherches cliniques de Montréal, Montreal, QC, H2W 1R7, Canada; †Department of Anatomy and Cell Biology, McGill University, Montreal, QC, H3A 2B2, Canada; and ‡Department of Medicine, University of Montreal, Montreal, QC, H3T 3J7, Canada

Submitted April 20, 2010; Revised June 8, 2010; Accepted June 16, 2010
Monitoring Editor: Benjamin Margolis

Dynamic regulation of cytoskeletal contractility through phosphorylation of the nonmuscle Myosin-II regulatory light chain (MRLC) provides an essential source of tension for shaping epithelial tissues. Rho GTPase and its effector kinase ROCK have been implicated in regulating MRLC phosphorylation in vivo, but evidence suggests that other mechanisms must be involved. Here, we report the identification of a single *Drosophila* homologue of the Death-associated protein kinase (DAPK) family, called Drak, as a regulator of MRLC phosphorylation. Based on analysis of null mutants, we find that Drak broadly promotes proper morphogenesis of epithelial tissues during development. Drak activity is largely redundant with that of the *Drosophila* ROCK orthologue, Rok, such that it is essential only when Rok levels are reduced. We demonstrate that these two kinases synergistically promote phosphorylation of Spaghetti squash (Sqh), the *Drosophila* MRLC orthologue, in vivo. The lethality of *drak/rok* mutants can be rescued by restoring Sqh activity, indicating that Sqh is the critical common effector of these two kinases. These results provide the first evidence that DAPK family kinases regulate actin dynamics in vivo and identify Drak as a novel component of the signaling networks that shape epithelial tissues.

INTRODUCTION

Regulation of cell shape is a fundamental mechanism for generating the complex forms of animal tissues. In epithelial tissues cellular processes such as apical constriction, transition between epithelial and mesenchymal states, and cell intercalation are spatially and temporally controlled to form and sculpt tissues in a variety of developmental contexts. Genetic analyses in model organisms ranging from flies and worms to mammals have shown that dynamic regulation of the actin cytoskeleton is a major driving force for reshaping epithelial cells and tissues (Quintin *et al*., 2008). In particular, cytoskeletal contractility resulting from the interaction of actin filaments with the molecular motor nonmuscle Myosin-II, the predominant form of Myosin in epithelial cells, provides an essential source of tensional forces in tissues (Lecuit and Lenne, 2007). Defining the signaling mechanisms governing Myosin activity is thus critical to understanding how cell and tissue shape is determined.

Actin-Myosin-II contractility is controlled primarily by reversible phosphorylation of the Myosin-II regulatory light chain (MRLC) (Vicente-Manzanares *et al*., 2009). Phosphorylation of MRLC at two sites (Thr-18 and Ser-19 in the human protein) promotes actin-activated Myosin GTPase activity, driving filament sliding (Sellers, 1985). The phosphorylation of these sites is subject to complex regulation. They can be phosphorylated by a number of different kinases including the prototypical Ca^{2+}/calmodulin-dependent Myosin light chain kinases (MLCK) (Gallagher *et al*., 1991). Furthermore, the activity of Myosin phosphatase, a PP1c-containing phosphatase holoenzyme, is specifically targeted to these sites by Myosin Phosphatase Targeting subunit (MYPT1) and related proteins, which are themselves subject to regulation by phosphorylation (Ito *et al*., 2004). This complexity suggests that multiple independent pathways feed into cytoskeletal regulation directly or indirectly through MRLC phosphorylation.

Rho-GTPase effector kinase (or ROCK) family kinases are the principal kinases implicated in regulating MRLC phosphorylation in developing epithelial tissues. Activation of Rho or ROCK in cells increases MRLC phosphorylation (Amano *et al*., 1996; Kimura *et al*., 1996; Kureishi *et al*., 1997; Ueda *et al*., 2002). In vivo, impairment of Rho GTPase signaling or of ROCK itself blocks morphogenetic processes during the embryonic development of both invertebrates and vertebrates (reviewed in [Quintin *et al*., 2008]). ROCK appears to act by two distinct mechanisms. ROCK can directly phosphorylate MRLC at both Thr-18 and Ser-19 in vitro (Amano *et al*., 1996; Ueda *et al*., 2002). It can also phosphorylate MYPT1, inhibiting myosin phosphatase activity and thereby indirectly increasing the level of phosphorylated MRLC (Kimura *et al*., 1996; Kawano *et al*., 1999). Although important, ROCK appears to be responsible for as little as 30% of MRLC phosphorylation activity in HeLa cells, suggesting that other mechanisms play a significant role (Ueda *et al*., 2002). There is strong evidence from studies in invertebrate systems that other mechanisms of MRLC phosphorylation are operative in epithelial tissues during development. In *Caenorhabditis elegans*, Myosin activity during embryo elongation is regulated by MRCK-1 and PAK-1, in addition to ROCK (Gally *et al*., 2009). In *Drosophila*, elimination of the single ROCK orthologue (Rok) in clones of epithelial cells in the developing eye and wing has surprisingly mild phenotypic effects. Although MRLC phosphory-

This article was published online ahead of print in *MBoC in Press* (http://www.molbiolcell.org/cgi/doi/10.1091/mbc.E10–04–0328) on June 23, 2010.

Address correspondence to: David R. Hipfner (david.hipfner@ircm.qc.ca).

lation is reduced in *rok* mutant cells a substantial amount remains, clearly pointing to the existence of one or more parallel mechanisms (Winter *et al*., 2001; Lee and Treisman, 2004; Corrigall *et al*., 2007; Escudero *et al*., 2007). However, in this case the identity of the kinase(s) responsible is not known.

Like ROCK, members of the Death-associated Protein Kinase (DAPK) family of Ser/Thr kinases can also phosphorylate MRLC. DAPKs form a subfamily of kinases with a close evolutionary relationship to MLCKs (Manning *et al*., 2002). All five mammalian DAPKs have some ability to phosphorylate MRLC on Ser-19 or both Thr-18 and Ser-19 in vitro (Cohen *et al*., 1997; Kogel *et al*., 1998; Sanjo *et al*., 1998; Kawai *et al*., 1999; Murata-Hori *et al*., 1999; Inbal *et al*., 2000). Two of these kinases (ZIPK and DAPK1) can also regulate MRLC phosphorylation in cells (Murata-Hori *et al*., 2001; Kuo *et al*., 2003). However, there is no indication, either from mouse knockouts or *C. elegans* DAPK mutants (of which all that have been analyzed are viable), that these kinases regulate MRLC or cytoskeleton dynamics in vivo (Raveh *et al*., 2001; Pelled *et al*., 2002; McGargill *et al*., 2004; Tong *et al*., 2009). A number of other potential substrates of these kinases involved in such diverse processes as apoptosis, chromatin regulation, splicing, translation, and membrane fusion have been identified (reviewed in [Bialik and Kimchi, 2006]), and it may be that one or more of these other substrates is of more importance to the physiological function of DAPKs. Alternatively, functional redundancy between the various DAPKs or between DAPKs and other kinases that phosphorylate MRLC may have obscured their requirement for Myosin regulation in vivo.

As reported below, we identified a single DAPK homologue (which we called Drak) encoded in the *Drosophila* genome, making flies a useful system for analyzing DAPK family kinase function in the absence of redundancy. *Drosophila* has proven to be extremely well-suited for studying actin cytoskeleton dynamics during tissue morphogenesis. A number of genetically tractable processes have been exploited for this purpose. For example, shortly after the transition from larval to pupal stages the epithelial tissues that give rise to the adult appendages (called imaginal discs) are remodeled to take on their adult forms in a process called imaginal disc eversion (Fristrom, 1988). During eversion the compact folded disc epithelia flatten and extend outwards along the proximal-distal axis, with the first, active phase of lengthening largely driven by flattening of the columnar epithelial cells (Condic *et al*., 1991). Drug inhibitor studies indicate that disc eversion is dependent on forces generated through the actin cytoskeleton (Fristrom and Fristrom, 1975; Chen *et al*., 2004). Consistent with this, mutations in genes encoding proteins involved in actin cytoskeleton regulation, including the *Drosophila* orthologues of RhoA (Rho1), ROCK (Rok), and nonmuscle Myosin II heavy and light chains (Zipper (Zip) and Spaghetti squash (Sqh), respectively), impair disc eversion, leading to a so-called "malformed" phenotype characterized by shorter, rounder wings, and shortened, misshapen third thoracic (T3) legs (Gotwals and Fristrom, 1991; Edwards and Kiehart, 1996; Halsell *et al*., 2000; Chen *et al*., 2004). Genetic studies have also implicated Rho GTPase signaling and nonmuscle Myosin II in a host of other morphogenetic processes in flies, including gastrulation, dorsal closure, head involution, tracheal morphogenesis, and morphogenetic furrow progression (reviewed in [Quintin *et al*., 2008]).

A number of the known molecules and regulatory relationships controlling Myosin-II activity in mammals are conserved in flies. Like its mammalian counterpart, Rok can directly phosphorylate MRLC/Sqh. It can also phosphorylate mammalian Mbs, a MYPT1-related protein, in vitro (Mizuno *et al*., 1999; Mizuno *et al*., 2002). Sqh phosphorylation is reduced in the absence of Rok and morphology of some epithelial tissues is disrupted (Lee and Treisman, 2004; Dawes-Hoang *et al*., 2005; Corrigall *et al*., 2007; Escudero *et al*., 2007). Conversely, loss of function mutations in the genes encoding Mbs or Flapwing (Flw), a PP1β that serves as the Myosin phosphatase catalytic subunit in *Drosophila*, lead to increased Sqh phosphorylation, which also affects epithelial tissue morphology (Lee and Treisman, 2004; Vereshchagina *et al*., 2004; Mitonaka *et al*., 2007). In this context, we have been characterizing the function of Drak. By analyzing null mutants, we find that Drak promotes proper morphogenesis of epithelial tissues during development, particularly of tissues whose form is generated by significant changes in cell shape and arrangement. It does so primarily by promoting Sqh phosphorylation in a manner that is largely redundant with Rok. Drak is thus a new component of the signaling networks that regulate the actin cytoskeleton to shape epithelial tissues.

MATERIALS AND METHODS

Fly Strains and Reagents

All crosses were performed at 25°C. flw^{GO172} (flw^{7}) is a strong hypomorphic allele. $rho1^{72O}$, rok^{2}, zip^{2}, flw^{GO172}, and Sb^{63b} are described in FlyBase and were obtained from the Bloomington *Drosophila* Stock Centre (Bloomington, IN). Transgenic flies expressing $Sqh^{E20/E21}$ and $Sqh^{A20/A21}$ under the control of the *sqh* promoter were kindly provided by R. Karess. *pBAC{WH}f07790* and *pBac{RB}e03054* were from the Exelixis Collection at Harvard Medical School (Thibault *et al*., 2004). The $drak^{del}$ deletion removes sequences located between *pBAC{WH}f07790* and *pBac{RB}e03054*, and was generated as described (Parks *et al*., 2004). The $drak^{KO}$ allele was generated by "ends-out" homologous recombination (Gong and Golic, 2003). To generate a targeting construct, upstream and downstream homology arm fragments of 3.94 and 3.46 kb, respectively, flanking exons 3–5 (which encode nearly the entire kinase domain) were PCR amplified and cloned into the pW25 vector. The resulting targeting construct was transformed into flies. After the crosses to generate potential recombinants, homologous recombination events were identified by Southern blot analysis (not shown). $drak^{del}$ and $drak^{KO}$ alleles are viable in both homozygous and transheterozygous combinations.

Sequence Analysis

Sequences used for multiple sequence alignments were: human nonmuscle Myosin light chain kinase (MYLK1) (RefSeq ID NP_444253.3); human skeletal muscle Myosin light chain kinase (MYLK2) (NP_149109.1); human cardiac Myosin light chain kinase (MYLK3) (NP_872299.2); human DAPK1 (NP_004929.2); human DAPK2 (NP_055141.2); human DAPK3/ZIPK (NP_001339.1); human DRAK1 (NP_004751.2); human DRAK2 (NP_004217.1); *Drosophila mealnogaster* Bent (NP_995598.1); *Drosophila* Stretchin-MLCK (AAF58090.2); *Drosophila* CG42347 (NP_610514.1); *Drosophila* Drak (NP_001162723.1). We note that there are two annotated exon 6 splice variants of *drak* in FlyBase. In one form (found in transcripts RA and RB), a short intron of 87 nucleotides in exon 6 is predicted to be excised, followed by exon 7 which contains a stop codon and 3′ untranslated region. In the other form (RC and RD), exon 6 is not spliced, and the open reading frame extends into the predicted intron, which contains a stop codon. The RA/RB and RC/RD forms thus encode proteins that differ in the C terminus, with RA/RB encoding a protein that is longer by 110 amino acids. Of two independent expressed sequence tags (ESTs) that we sequenced (RE12147 and GH05904, obtained from Drosophila Genomics Resource Center), we found only the RC/RD form, and we have used this for our analyses. Multiple sequence alignments and dendrogram were generated using Clustal-W. Pairwise sequence comparisons were performed with EMBOSS.

Antibodies and Immunostainings

Primary antibodies were as follows: alkaline phosphatase-coupled mouse anti-digoxigenin (Roche, Basel, Switzerland); mouse anti-Armadillo (N2 7A1) (Developmental Studies Hybridoma Bank); rabbit anti-Sqh (a kind gift from R. Karess [Jordan and Karess, 1997]); rabbit anti-cleaved Caspase 3 (#9661), rabbit anti-phospho-Myosin light chain 2 (Ser-19) (#3671), and rabbit anti-phospho-Ezrin/Radixin/Moesin (#3141) (Cell Signaling Technology, Beverly, MA). The MRLC phospho-Ser-19-specific antibody cross-reacts with *Drosophila* Sqh phosphorylated at the comparable residue, Ser-21. Tissues were immunostained as described (Hipfner *et al*., 2004).

Analysis of Tissue Extracts

For larval imaginal disc analyses, 10 wing/haltere/leg disc complexes of each genotype (15 for $drak^{del}$,rok^{2}/$drak^{KO}$) were dissected. For pupal samples, three to five pupae were collected at 4–6 h after puparium formation (APF). For embryo analyses, 40 embryos of the appropriate genotype were sorted at 12–16 h after egg laying (AEL) under a dissecting microscope to retain mutant embryos lacking GFP-marked balancer chromosomes (*FM7,Kr-GAL4,UAS-GFP* or *FM7,act::GFP*). Tissues were homogenized directly in SDS-PAGE sample buffer and heated at 80°C for 5 min before SDS-PAGE. Bands in immunoblots were quantified using the "Gel" function of ImageJ 1.42q.

RNA Interference in S2 Cells

Double-stranded RNAi was prepared and cells treated as described (Hipfner *et al.*, 2004). The templates were prepared using gene-specific PCR primers containing 5′ T7 and T3 promoter sequences to amplify sequences from exons 3–5 (oligos: 5′-AATTAACCCTCACTAAAGGGAGACAAGGAGATCAAGCACGAGA-3′ and 5′-TAATACGACTCACTATAGGGAGACACTGCGAGATGTTGAGGAA-3′), exon 6 (oligos: 5′-AATTAACCCTCACTAAAGGGAGAGAATGGCTCGGCAACGTCTGTCAAG-3′ and 5′-TAATACGACTCACTATAGGGAGAGGGACTTGAGCTCGGATTCGAAGTG-3′), or the 3′ untranslated region (oligos: 5′-AATTAACCCTCACTAAAGGGAGAT-

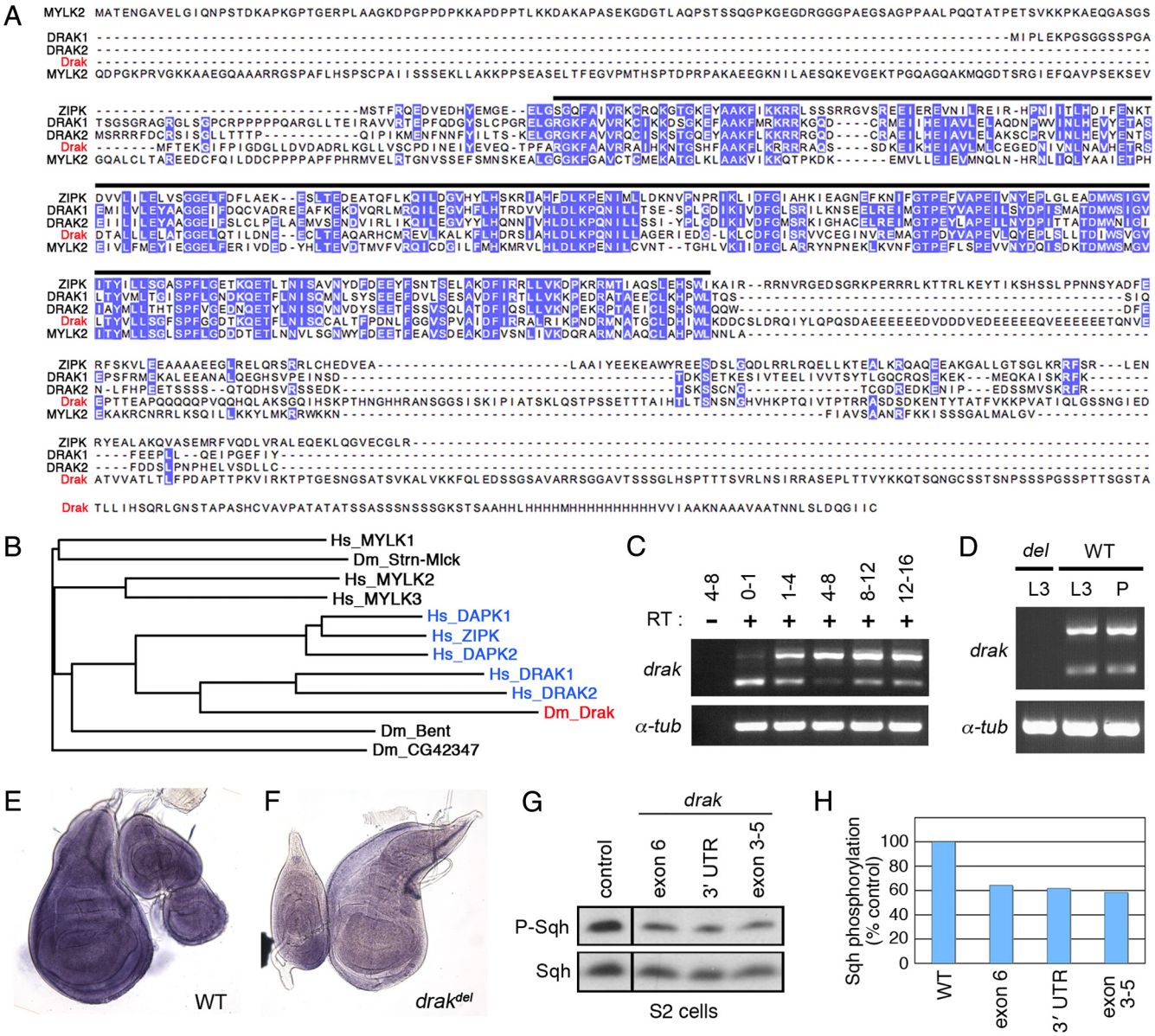

Figure 1. Drak is the single *Drosophila* homologue of DAPK family kinases. (A) Multiple sequence alignment of *Drosophila melanogaster* Drak with human DRAK1 and DRAK2, ZIPK, and skeletal muscle MLCK (MYLK2). Purple, identical amino acids conserved in at least three of the five sequences. Black bar, limits of the conserved kinase domains. (B) Dendrogram showing relation of Drak and other *Drosophila melanogaster* MLCK-like proteins to human DAPK (blue) and MLCK family kinases, based on alignment of kinase domain sequences. Hs_MYLK1, 2, and 3 correspond to nonmuscle, skeletal muscle, and cardiac Myosin light chain kinases. (C and D) Developmental time course analysis of *drak* expression by RT-PCR. RNA was from staged embryos (C) and third instar larval (L3) and pupal (P) wing discs (D). Numbers in C represent ages of the embryos in hours after egg laying. *drak* primers amplified two bands representing unspliced (upper) and spliced mRNA. Reverse transcriptase was left out of one reaction to confirm that both products derived from RNA and not contaminating genomic DNA. *α-tubulin84B* served as a positive control. (E and F) In situ hybridization analysis of *drak* expression in wing/leg/haltere imaginal discs from wild-type (E) and $drak^{del}$ mutant (F) animals. (G and H) Western blot analysis of lysates from S2 cells treated with dsRNAs targeting GFP (control) or three nonoverlapping regions of the *drak* transcript (exons 3–5, exon 6, and 3′ untranslated region), using anti-phospho-MRLC and anti-Sqh antibodies. Levels of phospho-Sqh, normalized to total Sqh levels, are plotted in H. Phospho-Sqh images are all from the same exposure of a single blot with intervening lanes removed, as are total Sqh images.

GGAGTTGGAACGGAATAGG-3′ and 5′-TAATACGACTCACTATAGGGAGAGCCATCGAAAAGGTCCAATA-3′) of the *drak* transcript. As a control, dsRNA was prepared from a template containing the EGFP coding sequence (oligos: 5′-AATTAACCCTCACTAAAGGGAGAGACGTAAACGGCCACAAGTT-3′ and 5′-TAATACGACTCACTATAGGGAGATGTTCTGCTGGTAGTGGTCG-3′).

RNA Analysis

For Northern blots, total RNA was isolated from 20 wild-type and homozygous *drak* mutant flies using Trizol reagent (Invitrogen, Carlsbad, CA). Ten micrograms of RNA was fractionated on a 1% agarose gel and transferred to nitrocellulose membrane. Blots were dried and UV-cross-linked and then probed with a random-primed ^{32}P-labeled probe generated from a full-length *drak* EST (RE12147). For RT-PCR, total RNA was extracted from frozen embryos or dissected larval/pupal discs using the RNeasy Mini Kit (Qiagen, Germantown, MD). Total RNA (0.5 μg) was used to synthesize the first strand cDNA using SuperScript II reverse transcriptase (Invitrogen). The PCR reaction was carried out according to standard procedures with an annealing temperature of 58°C and 30 cycles. The primers used spanned the first intron of *drak* (upper primer: 5′-AGAAGAGAAGCTGAGACGGAGTT-3′; lower primer: 5′-TCCACTTCGTAGATCTCGTTGAT-3′) or *a-tub84B* (upper primer: 5′-TTACGTTTGTCAAGCCTCATAGC-3′; lower primer: 5′-CTGAAGAAGGTGTTGAACGAGTC-3′).

Cuticle Preparations

Embryos were collected and processed according to standard methods. Devitellinized embryos were transferred to a drop of a 4:1 mixture of Hoyer's solution and lactic acid on a glass slide, coverslipped, and baked at 70°C overnight. Wings and legs were dissected in water, transferred into a drop of Fauré medium on microscope slides, coverslipped, and the coverslips kept pressed until dry. Wing areas were measured using ImageJ 1.42q.

RESULTS

Drak Is the Single Drosophila *Homologue of the DAPK Family of Kinases*

As a first step toward testing the potential involvement of *Drosophila* DAPK family members in tissue morphogenesis, we sought to identify fly homologues of these kinases. In BLAST searches for annotated fly proteins similar to human DAPKs and MLCKs, four kinase-domain-containing proteins were consistently ranked among the most similar (Stretchin-MLCK, Bent, and the annotated gene products CG42347 and CG32666). Phylogenetic analyses of either whole protein or kinase domain sequences placed one of these proteins, CG32666 (which we renamed Drak), in the DAPK family branch, which includes DAPK1, DAPK2, ZIPK, and DRAK1 and 2 (Figure 1, A and B). Drak most closely resembles members of the DRAK-like subgroup of DAPKs, consisting of an amino-terminal kinase domain with a longer nonconserved C-terminal tail containing no recognizable domains (Figure 1A). Based on pairwise sequence comparisons, Drak is most closely related to DRAK1, with 50% sequence identity and 72% similarity in the kinase domain. We conclude that Drak is the single fly DAPK family homologue.

drak is widely expressed during development. We detected *drak* transcripts by RT-PCR in very early (0 to 1 h

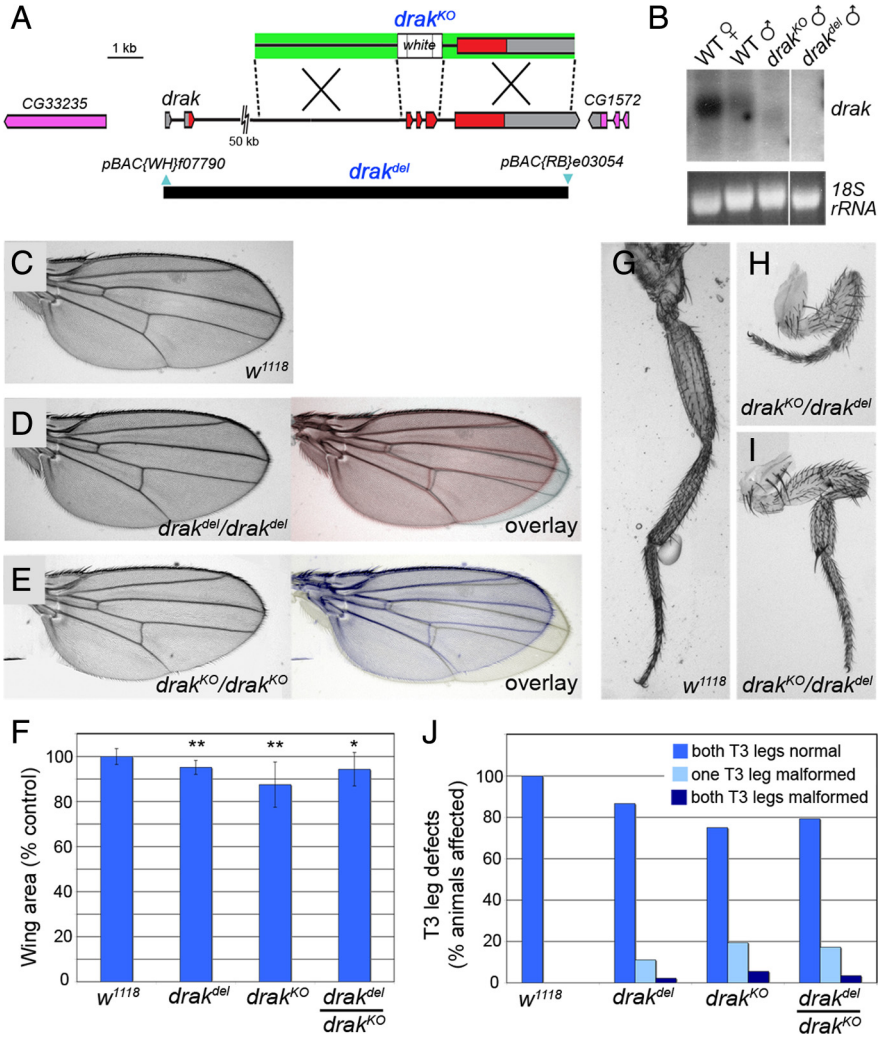

Figure 2. *drak* mutants have a "malformed' phenotype. (A) Map of the *drak* locus and defined deletions. The relative positions of noncoding (gray) and coding (red) exons of *drak* and the upstream (*CG33235*) and downstream (*CG1572*) neighboring genes are indicated. A schematic of the targeting construct used to generate the $drak^{KO}$ allele is shown above (arms of homology, green). The positions of the *piggyBac* insertions (blue) used to make the $drak^{del}$ allele and extent of the resulting deletion (black bar) are shown below. (B) Northern blot analysis of RNA extracted from w^{1118} female and male adult flies (WT), and $drak^{KO}$ and $drak^{del}$ mutant adult males. 18S rRNA was stained to ensure equal loading. Images are all from the same exposure of a single blot/gel with intervening lanes removed. (C–E) Wings from wild-type (C), $drak^{del}/drak^{del}$ (D), and $drak^{KO}/drak^{KO}$ (E) mutant flies. Overlays of *drak* mutant and wild-type wings are in color. (F) Areas of wild-type and *drak* mutant wings (average ± SD), based on measurement of 10 wings for each genotype. *t* test versus wild-type: *, $p < 0.05$; **, $p < 0.001$. (G–I) T3 legs from wild-type (G) and $drak^{KO}/drak^{del}$ (H and I) flies. (J) Quantification of frequency of malformed T3 leg phenotype in wild-type (n = 30), $drak^{del}/drak^{del}$ (n = 45), $drak^{KO}/drak^{KO}$ (n = 36), and $drak^{del}/drak^{KO}$ (n = 29) mutant flies.

AEL) *Drosophila* embryos, suggesting that a substantial amount of mRNA is maternally provided (Figure 1C). *drak* expression was detectable throughout the rest of embryogenesis and in wing imaginal discs from third instar larvae and pupae (Figure 1, C and D). The transcript was undetectable in animals homozygous for a deletion allele of the locus (see below) (Figure 1D). When assayed by in situ hybridization, *drak* expression appeared ubiquitous in third instar larval imaginal discs (Figure 1, E and F). This spatial and temporal distribution of *drak* is similar to that of the single DRAK orthologue in mice (Drak2), which is ubiquitously expressed in midgestation embryos (Mao *et al*., 2006) and is consistent with Drak having a general function.

As a first test to determine whether Drak has the capacity to regulate MRLC phosphorylation, we examined the effects of Drak depletion using specific double-stranded RNAs (dsRNA) on Sqh phosphorylation in *Drosophila* S2 cells. To control for the possibility of off-target effects, we tested dsRNAs targeting three distinct regions of the transcript. Compared with S2 cells treated with a control dsRNA, treatment with each of the three *drak* dsRNAs led to a reduction in phosphorylation of Sqh by 36–42% (Figure 1, G and H). Knockdown of Drak had little effect on total Sqh levels, indicating that the effects were posttranslational. Based on these observations, we considered Drak to be a good candidate for a MRLC kinase during development.

Drak Is a Novel "Malformed Class" Gene Controlling Adult Appendage Morphology

To study the physiological function of *drak*, we generated two molecularly-defined genomic deletions. In one approach, a pair of engineered transposable elements flanking *drak* were used to generate a chromosomal deletion ($drak^{del}$), which removes almost the entire gene without affecting any neighboring annotated genes (Figure 2A) (Parks *et al*., 2004). We also generated a targeted allele in which exons 3–5, encoding most of the kinase domain, were replaced with a *white* marker transgene by homologous recombination ($drak^{KO}$; Figure 2A) (Gong and Golic, 2003). In Northern blots we observed a transcript of reduced size in $drak^{KO}$ mutant adults and a loss of the transcript altogether in $drak^{del}$ mutants (Figure 2B). These observations are consistent with the molecular alterations in the two alleles and confirm that $drak^{del}$ is a null allele. We did not observe major differences in the behavior of $drak^{del}$ and $drak^{KO}$ alleles, suggesting that the targeted $drak^{KO}$ allele is also a functional null.

Animals homozygous for either allele were viable and fertile. We were able to maintain the *drak* alleles in homozygous stocks, indicating that *drak* is a nonessential gene in flies, as Drak2 is in mice (McGargill *et al*., 2004). Although viable, we observed morphological defects in the appendages of *drak* mutant flies. First, the mutants' wings were consistently smaller than those of wild-type controls, with a statistically significant decrease in average area of 5–13% in various experiments (Figure 2, C–F). The size reduction was not due to a generalized decrease in growth as we did not observe a reduction in body size. Rather, *drak* mutant wings were specifically shortened in the proximal-distal axis (Figure 2, C–E). Second, loss of *drak* led to a partially penetrant shortening of the legs, largely restricted to the T3 legs. Leg segments (primarily the femur and tibia) were shortened and abnormally bent (Figure 2, G–I). The percentage of flies with one defective T3 leg varied between 12 and 20%, with up to an additional 5% affected in both (Figure 2J). Comparable defects were rare in wild-type flies.

The defects in *drak* mutants are remarkably similar to those caused by impairment of imaginal disc eversion in

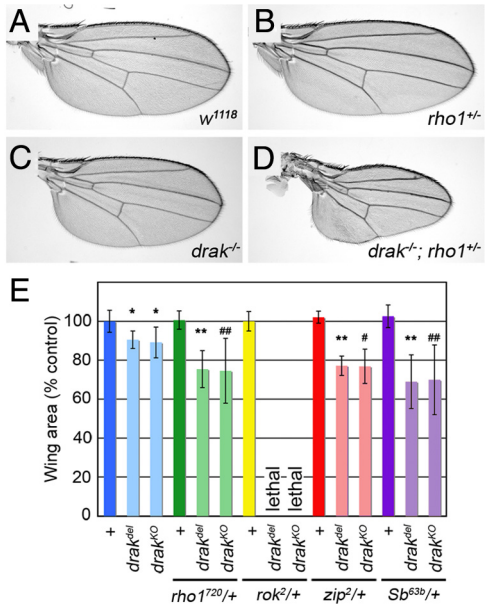

Figure 3. *drak* alleles interact genetically with malformed class genes. (A–D) Wings from w^{1118}/Y (WT) (A), $rho1^{A720}/+$ (B), $drak^{del}/Y$ (C), and $drak^{del}/Y$; $rho1^{A720}/+$ (D) flies. (E) Quantification of wing areas (average ± SD) from wild-type and *drak* mutant flies heterozygous for various malformed-class genes. Twelve wings were measured for each genotype. *, significantly different from w^{1118} ($p < .001$); **, significantly different from $drak^{del}$ ($p < .001$); #, significantly different from $drak^{KO}$ ($p < .05$); ##, significantly different from $drak^{KO}$ ($p < .002$). Note that *drak* mutant rok^{2} heterozygous adults were never recovered.

malformed class mutants. Malformed mutations cause synthetic phenotypes in double heterozygotes, suggesting that disc eversion is particularly sensitive to changes in cytoskeleton regulation (Halsell *et al*., 2000; Bayer *et al*., 2003; Chen *et al*., 2004). To determine whether Drak is a component of the signaling pathways regulating disc eversion, we tested whether the *drak* mutant phenotypes could be enhanced by heterozygosity for known malformed mutations. Whereas wings from $rho1^{72O}$ heterozygous males were wild-type in size and shape and $drak^{del}$ male wings were significantly shorter, the combination of the two in $drak^{del}/Y;rho1^{72O}/+$ flies caused a significant further reduction in size ($p < .001$) (Figure 3, A–E). Wings from these animals were frequently severely shortened and misshapen (Figure 3D). Similar genetic interactions were observed with both *drak* alleles and between *drak* and other malformed class genes, including *Stubble/stubbloid* (*Sb/sbd*, encoding a transmembrane protease) (Beaton *et al*., 1988) and *zip* (Figure 3E) (Halsell *et al*., 2000). Interestingly, we never recovered animals mutant for *drak* and heterozygous for a mutant allele of *rok*, although *rok* heterozygotes alone were normal (Figure 3E and data not shown). This synthetic lethality suggested that these two kinases act redundantly in some essential process. Based on these genetic interactions, we conclude that *drak* is a novel malformed class gene required for normal imaginal disc eversion.

Drak and Rok Have Overlapping Functions in Epithelial Tissue Morphogenesis

To identify the redundant functions of Drak and Rok, we analyzed $drak^{-/-},rok^{+/-}$ animals. $drak^{-/-},rok^{+/-}$ embryos hatched to form grossly normal looking larvae. However, at

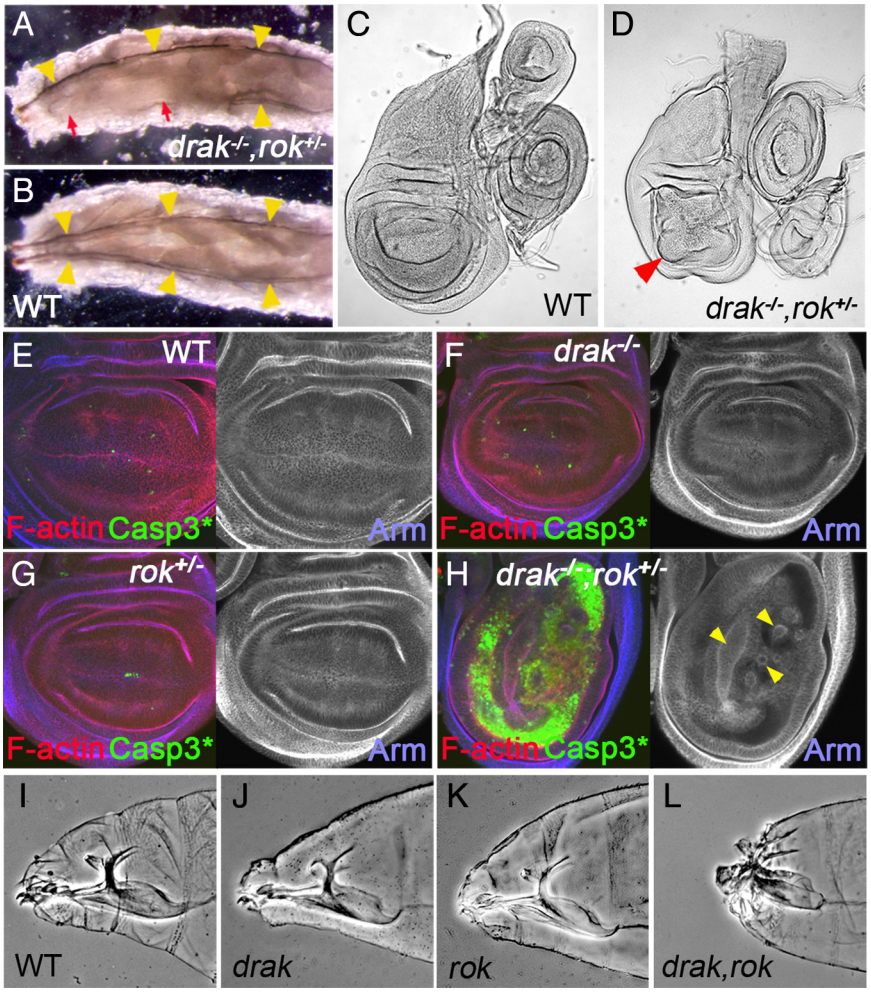

Figure 4. Drak and Rok have partly redundant functions during development. (A and B) Dorsal views of $drak^{del}$,rok^{2}/$drak^{del}$ (A) and wild-type (B) third instar larvae. The bilaterally symmetrical main dorsal trunks of the tracheal system are indicated by yellow arrowheads. Portions of the dorsal tracheal trunks are frequently absent in $drak^{del}$,rok^{2}/$drak^{del}$ mutants (A, red arrows). (C and D) Wings imaginal discs from wild-type (w^{1118}) (C) and $drak^{del}$,rok^{2}/$drak^{KO}$ (D) third instar larvae. Red arrowhead indicates distorted wing pouch. (E–H) Third instar wing imaginal discs from wild-type (E), $drak^{del}$/$drak^{KO}$ (F), rok^{2}/+ heterozygous (G), and $drak^{del}$,rok^{2}/$drak^{KO}$ (H) animals. Apoptotic cells are stained with an antibody recognizing activated Caspase-3 (green), F-actin is stained with phalloidin (red), and Armadillo is stained blue. (I–L) Anterior regions of wild-type (I), $drak^{del}$ (J), rok^{2}/Y (K), and $drak^{del}$,rok^{2}/Y (L) embryonic cuticles.

later time points it became apparent that more than half of the larvae were missing random segments of the tracheal tree (Figure 4A). These defects were not observed in wild-type, $rok^{+/-}$, or *drak* mutant larvae (Figure 4B and data not shown). The tracheal tree is formed by epithelial cells which undergo a series of changes in cell shape, migrations, and rearrangements (Cabernard *et al*., 2004). The tracheal defects suggested that *drak* and *rok* may be redundantly required for one or more of these processes.

Imaginal discs isolated from $drak^{-/-}$,$rok^{+/-}$ third instar larvae appeared grossly normal, except for the wing pouch region of wing discs which were abnormally folded and distorted (Figure 4, C and D). The wing discs were very similar in appearance to those from animals with lack of function mutations in any of several different genes required for epithelial integrity (e.g., Dearolf *et al*., 1988; Speck *et al*., 2003; Hipfner *et al*., 2004). Impaired epithelial integrity results in high levels of apoptosis as cells sort out of the epithelial layer (Brumby and Richardson, 2003; Hipfner *et al*., 2004). To see whether epithelial integrity was compromised in $drak^{-/-}$,$rok^{+/-}$ animals, we stained imaginal discs to reveal filamentous actin, Armadillo (Arm, which marks the apical adherens junctions), and activated Caspase-3 (which selectively stains apoptotic cells). Discs from *drak* mutants or *rok* heterozygotes looked morphologically normal and had levels of apoptosis comparable to wild-type (Figure 4, E–G). In contrast, wing discs from $drak^{-/-}$,$rok^{+/-}$ animals were composed of unusually thin epithelial layers, which were grossly distorted (Figure 4H). In the wing pouch, folds projecting basally out of the plane of the epithelium were observed (Figure 4H, arrowheads). These distortions were accompanied by massive apoptosis (Figure 4H), with the loss of cells likely accounting for reduced epithelial thickness. These observations suggest that Drak and Rok are redundantly required for maintenance of wing disc epithelium integrity.

To see whether Drak is involved in morphogenesis of epithelial tissues at earlier stages, we examined *drak,rok* double null mutant embryos. 86% of *rok* mutant embryos hatched into normal looking first instar larvae (n = 111), which survived for some time without progressing beyond second instar before dying (data not shown) (Winter *et al*., 2001). *drak* mutant embryos were also morphologically normal (data not shown). In contrast, 100% of $drak^{-/-}$,$rok^{-/-}$ embryos died before hatching. Double mutants showed a fully penetrant head defect, characterized by an anterior hole in the embryonic cuticle and anterior malformations of the cephalopharyngeal skeleton, which was not observed in either single mutant alone (Figure 4, I–L). These phenotypes are characteristic of a failure in head involution, the process by which dorsal and lateral epidermal cells spread to cover the anterior end of the embryo (VanHook and Letsou, 2008). Taken together, our genetic analyses suggest that Drak and Rok redundantly regulate epithelial morphogenesis in multiple developmental contexts.

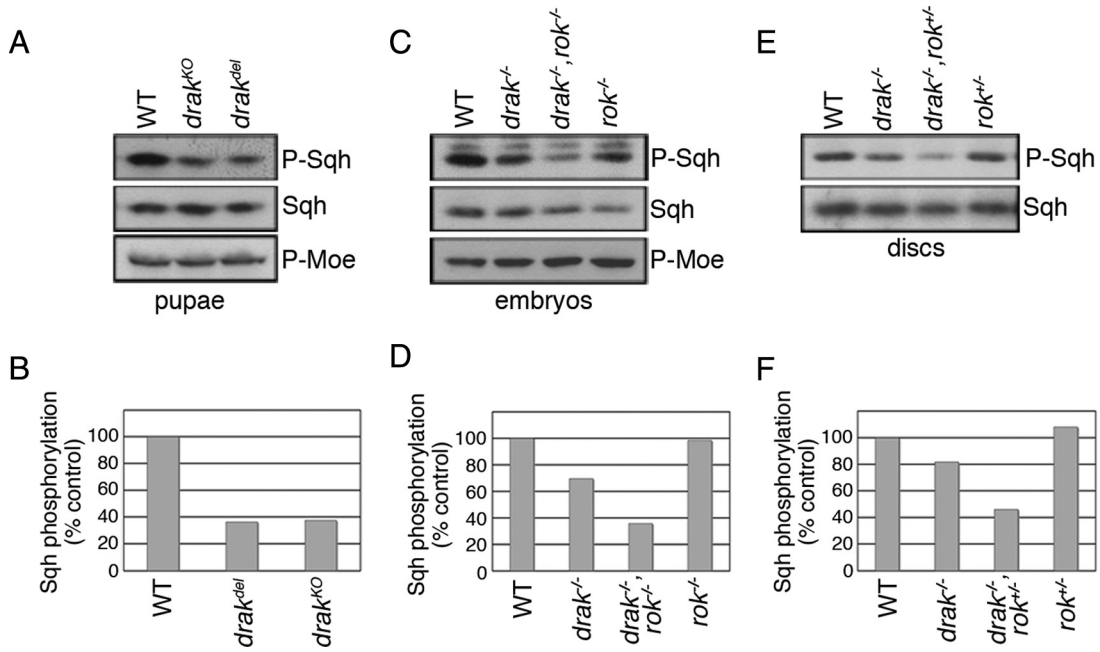

Figure 5. Drak and Rok both regulate Sqh phosphorylation. (A and B) Western blot analysis of 4–6 h APF pupal lysates prepared from wild-type (WT), $drak^{KO}$, and $drak^{del}$ pupae, using anti-phospho-MRLC, anti-phospho-Moesin, and anti-Sqh antibodies. Levels of phospho-Sqh, normalized to total Sqh levels, are plotted in (B). (C and D) Western blot analysis of dorsal closure-stage wild-type, $drak^{del}$, rok^2, and $drak^{del}$,rok^2 double mutant embryo lysates, using anti-phospho-MRLC, anti-phospho-Moesin, and anti-Sqh antibodies. Levels of phospho-Sqh, normalized to total Sqh levels, are plotted in (D). (E and F) Western blot analysis of third instar wing imaginal disc lysates prepared from wild-type, $drak^{del}/drak^{KO}$, $rok^2/+$, and $drak^{del}$,$rok^2/drak^{KO}$ larvae, using anti-phospho-MRLC and anti-Sqh antibodies. Levels of phospho-Sqh, normalized to total Sqh levels, are plotted in (F).

Drak and Rok Act Synergistically to Promote Sqh Phosphorylation

Having shown that Drak promotes Sqh/MRLC phosphorylation in cultured cells (Figure 1G), we wondered whether the same was true in vivo. We tested whether Sqh phosphorylation is altered in pupae undergoing disc eversion. In Western blots of whole pupal extracts, the levels of phospho-Sqh were reduced by more than 60% in $drak^{del}$ and $drak^{KO}$ mutants relative to wild-type (Figure 5, A and B). Total Sqh levels were essentially unchanged. Thus, Drak promotes Sqh phosphorylation in vivo. As a control for specificity, we also examined phosphorylation of Moesin, a cytoskeletal linker protein whose phosphorylation appears to be coupled to that of Myosin in some circumstances (Fukata *et al*., 1998; Grusche *et al*., 2009). Unlike Sqh, Moesin phosphorylation levels were unchanged in *drak* mutants (Figure 5A). Thus, there is specificity to the effects on Sqh phosphorylation.

The most straightforward explanation for the redundancy between Drak and Rok is that they regulate a common target. We examined phospho-Sqh levels in single and double mutants. Compared with wild-type controls, the levels of Sqh phosphorylation were 30% lower in 12- to 16-h-old *drak* mutant embryos (Figure 5, C and D). Phospho-Sqh levels were only slightly (2%) reduced in rok^2 homozygous mutant embryos. In embryos homozygous for both mutations, however, phospho-Sqh levels were further reduced to just 36% of wild-type controls, indicating that removal of the two kinases has synergistic effects on Sqh phosphorylation. Moesin phosphorylation was again unaffected (Figure 5C). $drak^{-/-}$,$rok^{+/-}$ larval wing discs showed a similar synergistic reduction in Sqh phosphorylation relative to $drak^{-/-}$ and $rok^{+/-}$ discs alone (Figure 5, E and F). Thus, Drak and Rok activities specifically intersect at the level of Sqh phosphorylation at multiple developmental stages. The synergistic nature of the interaction between *drak* and *rok* null alleles, both at phenotypic and molecular levels, suggests that these two kinases likely act through parallel but convergent pathways to promote Sqh phosphorylation (Perez-Perez *et al*., 2009).

Sqh Is the Main Physiological Target of Drak

The phenotypes we observe in *drak* and *drak/rok* mutant animals are consistent with Drak regulating Sqh phosphorylation and actomyosin contractility during processes involving significant reorganization of epithelial cells. However, Drak could have other targets. To see whether Sqh is the critical physiological target of Drak, we examined the effects of manipulating Sqh activity in *drak* mutants by two means. Sqh phosphorylation is normally counteracted by Flw, the *Drosophila* Myosin phosphatase. *flw* mutants have increased levels of Sqh phosphorylation, and the lethality of strong hypomorphic alleles can be rescued by manipulations that reduce phospho-Sqh levels or Myosin activity. This indicates that Sqh is the critical essential target of this phosphatase in vivo (Vereshchagina *et al*., 2004). We reasoned that if Sqh is also the main downstream target of Drak, either directly or indirectly, then reducing Flw activity should rescue *drak* mutant defects and vice-versa. To test this, we performed epistasis experiments using our *drak* alleles and flw^{G0172}, a semilethal allele (Vereshchagina *et al*., 2004). More than 99% of flw^{GO172} mutants died before reaching adulthood, and the few escapers that hatched all had curled or crumpled wings (Figure 6, A and B). As we predicted, simultaneous elimination of *drak* fully rescued both the lethality and wing phenotype of flw^{GO172} mutants (Figure 6, A and C). All *drak*,*flw* double mutants had normal T3 leg morphology (Figure 6D), indicating that reduction of *flw*

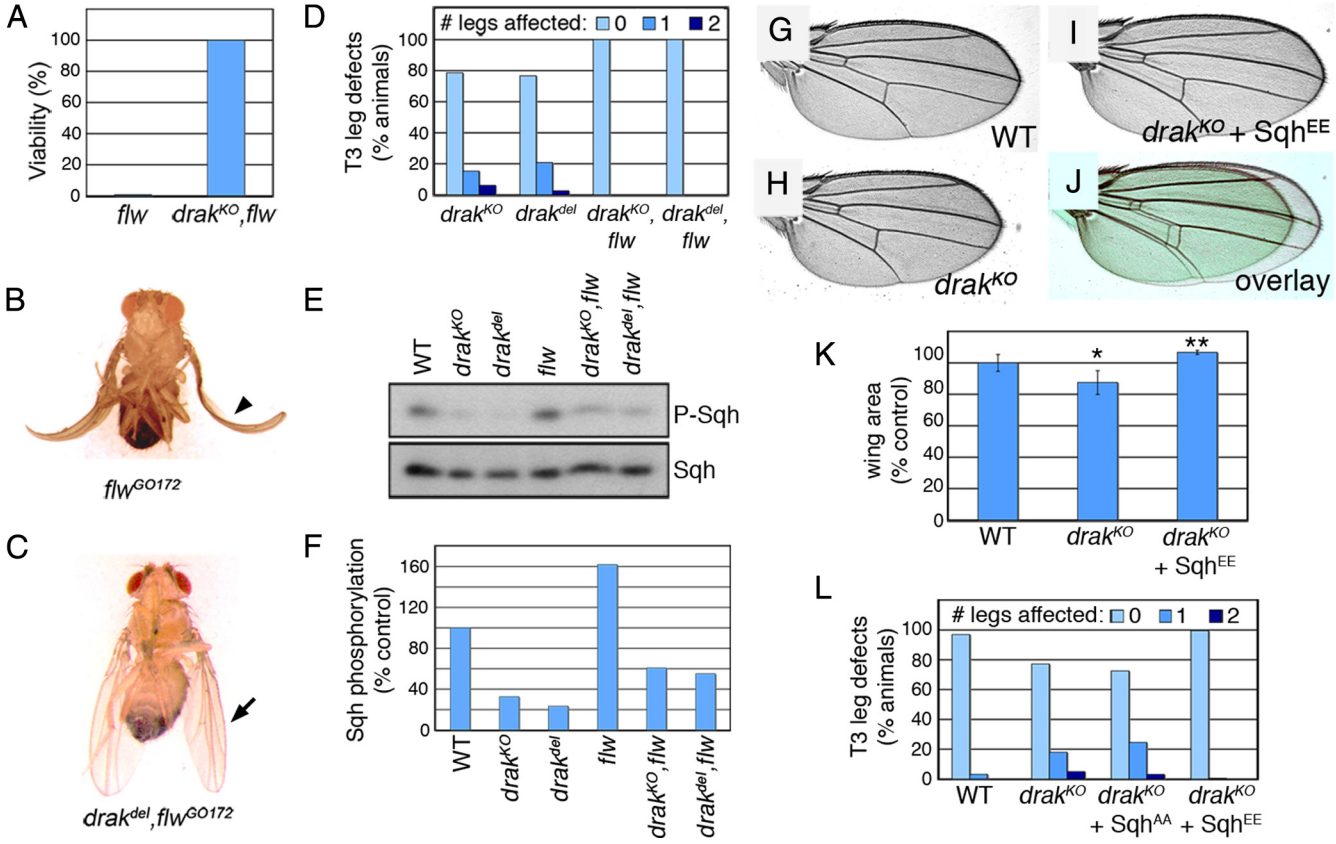

Figure 6. Increasing Sqh activity rescues *drak* mutant phenotypes. (A) Plot of the viability of flw^{GO172}/Y (expected n = 137) and $drak^{KO},flw^{GO172}/Y$ (n = 79) flies. (B) flw^{GO172}/Y fly, showing abnormal curled wing phenotype of rare *flw* adult escapers (arrowhead). (C) $drak^{del},flw^{GO172}/Y$ fly, with normal wing morphology (arrow). (D) Quantification of leg defects in $drak^{KO}/Y$ (n = 77), $drak^{del}/Y$ (n = 98), $drak^{KO},flw^{GO172}/Y$ (n = 66), and $drak^{del},flw^{GO172}/Y$ (n = 135) flies. (E and F) Western blot analysis of third instar wing imaginal disc lysates prepared from wild-type, $drak^{KO}/Y$, $drak^{del}/Y$, flw^{GO172}/Y, $drak^{KO},flw^{GO172}/Y$, and $drak^{del},flw^{GO172}/Y$ larvae, using anti-phospho-MRLC and anti-Sqh antibodies. Levels of phospho-Sqh, normalized to total Sqh levels, are plotted in F. (G–I) Wings from wild-type (G), $drak^{KO}/Y$ (H), and $drak^{KO}/Y;Sqh^{EE}/+$ (I) flies. Wings closest to the mean measured wing areas for each genotype were chosen. (J) Overlay of wings in H and I, false colored green and red, respectively. (K) Measurements of wing areas (average ± SD). n = 12 for each genotype. *, significantly different from wild-type ($p < .001$). **, significantly different from $drak^{KO}/Y$ ($p < 0.001$). (L) Quantification of leg defects in wild-type (n = 96), $drak^{KO}/Y$ (n = 223), $drak^{KO}/Y;Sqh^{AA}/+$ (n = 98), and $drak^{KO}/Y;Sqh^{EE}/+$ (n = 215) flies.

restored disc eversion to normal in the absence of Drak. This mutual phenotypic rescue was reflected at the level of Sqh phosphorylation in wing imaginal discs. Phospho-Sqh levels were higher than normal in *flw* mutant discs, reduced in *drak* mutants, and intermediate in the *drak,flw* double mutants (Figure 6, E and F). The opposing effects of mutations at these two loci indicate that both Flw and Drak regulate Sqh phosphorylation and are consistent with Sqh being an important physiological target of both proteins.

In a second approach, we tested the ability of constitutively active Sqh to rescue *drak* mutant phenotypes. $Sqh^{E20/E21}$ (Sqh^{EE}) is a phosphomimetic form of Sqh, in which the critical Thr and Ser residues responsible for Sqh activation have been mutated to glutamate (Jordan and Karess, 1997). Transgenic expression of Sqh^{EE} under the control of the endogenous *sqh* promoter rescued the short wing phenotype of *drak* mutants (Figure 6, G–K). Sqh^{EE} also completely suppressed the appearance of malformed legs in *drak* mutants (Figure 6L). This was dependent upon Sqh activation, as comparable expression of the nonactivatable mutant form $Sqh^{A20/A21}$ (Sqh^{AA}) had no effect (Figure 6L). Together, these results indicate that Sqh is the main effector of Drak.

Sqh Is the Common Physiological Effector of Both Drak and Rok

Sqh has also been proposed to be the principal downstream target of Rok in flies (Winter *et al.*, 2001). To see whether reduced Sqh phosphorylation is the cause of lethality in $drak^{-/-}$, $rok^{+/-}$ animals, we performed similar rescue experiments. Strong reduction of Flw activity counteracted the effects of Drak and Rok loss/reduction, as 77% of $drak^{-/-},flw^{-/-},rok^{+/-}$ animals (66 of 86 expected) survived to adulthood (Figure 7A). This suggests that it is low levels of Sqh activity that kill $drak^{-/-}$, $rok^{+/-}$ animals. Consistent with this, directly restoring Sqh activity by expressing Sqh^{EE} almost completely rescued the viability of $drak^{-/-}$, $rok^{+/-}$ animals (131 of 159 expected) (Figure 7A). Most of the rescued animals were normal in appearance (Figure 7B). The rescue was already apparent in third instar wing discs, which were no longer distorted and contained many fewer activated Caspase-3–positive apoptotic cells (Figure 7C). This was dependent upon Sqh activation, as Sqh^{AA} did not improve adult viability (Figure 7A) or the appearance of $drak^{-/-}$, $rok^{+/-}$ discs (Figure 7D). These results confirm that insufficient Sqh phosphorylation is the principal cause of lethality when both Drak and Rok levels

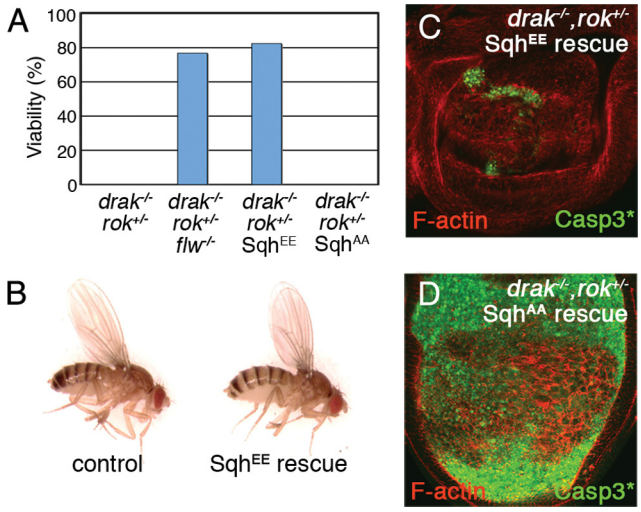

Figure 7. Sqh is the critical target downstream of Drak and Rok. (A) Plot of adult fly viability. Genotypes were as follows: $drak^{del}$,rok^{2}/$drak^{KO}$ (0/90 expected); $drak^{del}$,flw^{GO172},rok^{2}/$drak^{KO}$,flw^{GO172} (66/86 expected); $drak^{del}$,rok^{2}/$drak^{KO}$; Sqh^{EE}/+ (131/159 expected); and $drak^{del}$,rok^{2}/$drak^{KO}$; Sqh^{AA}/+ (0/49 expected). (B) Pictures of $drak^{KO}$/+;Sqh^{EE}/+ (control) and $drak^{del}$,rok^{2}/$drak^{KO}$; Sqh^{EE}/+ (Sqh^{EE} rescue) sibling flies. (C and D) Third instar wing imaginal discs from $drak^{del}$,rok^{2}/$drak^{KO}$; Sqh^{EE}/+ (C) and $drak^{del}$,rok^{2}/$drak^{KO}$; Sqh^{AA}/+ (D) animals, stained to reveal activated Caspase-3 (green) and F-actin (red).

are reduced. Together, our results support a model in which Drak and Rok act in parallel pathways to promote Sqh phosphorylation, and thus actomyosin contractility, during epithelial tissue morphogenesis.

DISCUSSION

Regulation of actin cytoskeleton contractility through nonmuscle Myosin II phosphorylation provides an essential means of controlling tensional forces during the morphogenesis of epithelial tissues. Previous studies have demonstrated a conserved requirement for Rho GTPases and ROCK in MRLC phosphorylation in vivo (Quintin *et al.*, 2008). However, this function is not exclusive to the Rho-ROCK signaling cassette. In particular, genetic evidence in *C. elegans* and *Drosophila* points to the existence of parallel mechanisms for regulating MRLC phosphorylation in developing epithelia, involving MRCK-1 and PAK-1 in worms and one or more unknown kinases in flies (Lee and Treisman, 2004; Corrigall *et al.*, 2007; Escudero *et al.*, 2007; Gally *et al.*, 2009). Our characterization of flies lacking Drak, the single DAPK family kinase in *Drosophila*, clearly demonstrate that this kinase regulates Sqh/MRLC phosphorylation in parallel to Rok and identify it as a novel component in the signaling pathways regulating epithelial tissue morphogenesis.

Drak Regulates Sqh Phosphorylation

Based on both morphological criteria and genetic interactions, *drak* is a malformed class gene required for normal imaginal disc eversion. Disc eversion is a Rho GTPase and actin-dependent process (Fristrom and Fristrom, 1975; Edwards and Kiehart, 1996; Halsell *et al.*, 2000; Chen *et al.*, 2004). In addition to regulating gene expression, signaling by Rho through Rok and Sqh/MRLC is thought to trigger actomyosin contractility needed for the extensive cell flattening that occurs (Condic *et al.*, 1991; Chen *et al.*, 2004). This is consistent with the observation that partial reduction of Sqh levels is sufficient to cause leg and wing malformation (Edwards and Kiehart, 1996). We found that the wing and leg defects in *drak* mutants were accompanied by a substantial decrease in Sqh phosphorylation in pupae undergoing eversion. This was not just correlated with but actually caused the disc eversion defects, as expression of a phosphomimetic form of Sqh but not a nonphosphorylatable form restored appendage morphology to normal. Thus, the principal function of Drak in imaginal disc eversion is to promote Sqh phosphorylation.

Drak is broadly expressed throughout development. Although we did not observe other morphological defects in *drak* mutants, phospho-Sqh levels were reduced in all tissues examined. The specific requirement of *drak* for imaginal disc eversion and not other processes suggests that eversion may require more extensive Sqh phosphorylation, consistent with the known sensitivity of the process to genetic manipulation (Edwards and Kiehart, 1996; Halsell *et al.*, 2000; Chen *et al.*, 2004). It is worth noting that this function is not limited to epithelia, as ~40% of Sqh phosphorylation in cultured S2 cells (which are thought to be of hemocyte origin) depends on Drak.

Partially Redundant Functions of Drak and Rok in Epithelial Tissue Morphogenesis

Drak and Rok have partially redundant or overlapping functions. Although *rok* heterozygotes are phenotypically normal, removing just one functional copy of *rok* in a *drak* mutant background leads to fully-penetrant lethality. Both $drak^{-/-}$;$rok^{+/-}$ and $drak^{-/-}$;$rok^{-/-}$ animals show morphological defects that are not present in either single mutant alone. Both kinases play a role in shaping imaginal disc epithelia, as $drak^{-/-}$;$rok^{+/-}$ discs show morphological defects and massive apoptosis. Interestingly, mutations in the genes encoding Moesin, a protein that links the actin cytoskeleton to membrane proteins, and its activating kinase Slik both have remarkably similar consequences on disc morphology and apoptosis, reflecting a failure in epithelial integrity (Speck *et al.*, 2003; Hipfner *et al.*, 2004). We did not observe reductions in Moesin phosphorylation in *drak* or *drak/rok* mutants, ruling this out as a possible cause of the defect. It may be that reduced anchoring of the actin cytoskeleton and reduction of actomyosin contractility both have the same consequence on disc morphology, in that both impair the ability of cells to generate tension. *drak,rok* double mutants also fail to complete head involution and have problems with formation of the tracheal tree. The processes that are impaired in *drak,rok* mutants (head involution, tracheal morphogenesis, disc eversion) all involve dramatic changes in cell shape (Condic *et al.*, 1991; Cabernard *et al.*, 2004; VanHook and Letsou, 2008). This spectrum of phenotypes suggests that Drak, like Rok, is broadly involved in the dynamic changes in epithelial cell organization that accompany tissue morphogenesis.

Although Rok appears to be the predominant kinase in many morphogenetic processes, our genetic analyses indicate that Drak also compensates for the absence of Rok, though to a lesser extent. For example, the fully-penetrant head involution defect in $drak^{-/-}$;$rok^{-/-}$ embryos is not observed in *rok* mutants alone, indicating that Drak can partially substitute for Rok in this process. Similarly, the relatively mild phenotype associated with *rok* mutant wing imaginal disc clones (Winter *et al.*, 2001) compared with the dramatic loss of epithelial integrity observed in $drak^{-/-}$;$rok^{+/-}$ wing discs suggests that *drak* compensates to a large extent for the loss of Rok in this tissue.

The synergistic nature of the interaction between *drak* and *rok* is reflected at molecular as well as phenotypic levels. In both embryos and wing imaginal discs, simultaneous reduction of *drak* and *rok* leads to a synergistic decrease in Sqh phosphorylation. It is this reduction in Sqh phosphorylation rather than misregulation of other potential targets that causes the morphogenetic defects, as expression of the phosphomimetic form of Sqh rescued the viability and morphology of $drak^{-/-};rok^{+/-}$ animals. It remains to be seen how the activity of Drak and Rok are temporally and spatially integrated to control Sqh activity within cells and more broadly within tissues. Mammalian ROCK1 can phosphorylate ZIPK at two sites in vitro, promoting its catalytic activity (Hagerty *et al*., 2007). However, neither site is conserved in Drak. The fact that reducing *rok* gene dosage has such a strong phenotypic effect in the absence of Drak suggests that the primary effect of Rok on Sqh phosphorylation in vivo is unlikely to involve direct regulation of Drak. The synergistic nature of the genetic interactions is more consistent with a model in which Drak and Rok act through parallel but convergent signaling pathways (Perez-Perez *et al*., 2009). This convergence could be at the level of several different targets identified as potential substrates of both ROCK and DAPK family kinases in mammals, including Sqh/MRLC, MYPT1, and CPI-17, although the ultimate common effector of both kinases is Sqh/MRLC. Studies of MLCK, ROCK, and DAPK1 in cells suggest that these kinases regulate distinct pools of MRLC. Interestingly, whereas MLCK regulates the formation of cortical actin bundles, both ROCK and DAPK1 control assembly of more centrally-located stress fibers (Totsukawa *et al*., 2000; Katoh *et al*., 2001; Kuo *et al*., 2003), and overexpression of DAPK1 can overcome cell morphology defects caused by treatment of cells with a ROCK inhibitor (Borman *et al*., 2002). Overlapping subcellular distribution of Rok and Drak could also explain, at least in part, the partial functional redundancy between these kinases.

Our results represent the first evidence for the involvement of DAPK family kinases in actin cytoskeleton regulation in vivo. Given the ability of mammalian DAPKs to phosphorylate MRLC, it is likely to be a physiologically important target of at least some of the mammalian kinases during tissue morphogenesis as well. However, our results indicate that the analysis of the functions of mammalian DAPKs in vivo may be complicated not only by redundancy between DAPK family members but also with ROCKs.

ACKNOWLEDGMENTS

We thank Roger Karess for generously providing reagents, Jean-François Côté and Nicholas Harden for helpful comments on the manuscript, and Karen Oh and Gregory Cormack for expert technical assistance. This work was supported by Canadian Institutes of Health Research grant #81187. D.R.H. is supported by a 'Junior II' Research Scholarship from Fonds de la recherche en santé Québec.

REFERENCES

Amano, M., Ito, M., Kimura, K., Fukata, Y., Chihara, K., Nakano, T., Matsuura, Y., and Kaibuchi, K. (1996). Phosphorylation and activation of myosin by Rho-associated kinase (Rho-kinase). J. Biol. Chem. *271*, 20246–20249.

Bayer, C. A., Halsell, S. R., Fristrom, J. W., Kiehart, D. P., and von Kalm, L. (2003). Genetic interactions between the RhoA and Stubble-stubbloid loci suggest a role for a type II transmembrane serine protease in intracellular signaling during Drosophila imaginal disc morphogenesis. Genetics *165*, 1417–1432.

Beaton, A. H., Kiss, I., Fristrom, D., and Fristrom, J. W. (1988). Interaction of the Stubble-stubbloid locus and the Broad-complex of *Drosophila melanogaster*. Genetics *120*, 453–464.

Bialik, S., and Kimchi, A. (2006). The death-associated protein kinases: structure, function, and beyond. Annu. Rev. Biochem. *75*, 189–210.

Borman, M. A., MacDonald, J. A., Muranyi, A., Hartshorne, D. J., and Haystead, T. A. (2002). Smooth muscle myosin phosphatase-associated kinase induces Ca2+ sensitization via myosin phosphatase inhibition. J. Biol. Chem. *277*, 23441–23446.

Brumby, A. M., and Richardson, H. E. (2003). scribble mutants cooperate with oncogenic Ras or Notch to cause neoplastic overgrowth in Drosophila. EMBO J. *22*, 5769–5779.

Cabernard, C., Neumann, M., and Affolter, M. (2004). Cellular and molecular mechanisms involved in branching morphogenesis of the Drosophila tracheal system. J. Appl. Physiol. *97*, 2347–2353.

Chen, G. C., Gajowniczek, P., and Settleman, J. (2004). Rho-LIM kinase signaling regulates ecdysone-induced gene expression and morphogenesis during Drosophila metamorphosis. Curr. Biol. *14*, 309–313.

Cohen, O., Feinstein, E., and Kimchi, A. (1997). DAP-kinase is a Ca2+/calmodulin-dependent, cytoskeletal-associated protein kinase, with cell death-inducing functions that depend on its catalytic activity. EMBO J. *16*, 998–1008.

Condic, M. L., Fristrom, D., and Fristrom, J. W. (1991). Apical cell shape changes during Drosophila imaginal leg disc elongation: a novel morphogenetic mechanism. Development *111*, 23–33.

Corrigall, D., Walther, R. F., Rodriguez, L., Fichelson, P., and Pichaud, F. (2007). Hedgehog signaling is a principal inducer of Myosin-II-driven cell ingression in Drosophila epithelia. Dev. Cell *13*, 730–742.

Dawes-Hoang, R. E., Parmar, K. M., Christiansen, A. E., Phelps, C. B., Brand, A. H., and Wieschaus, E. F. (2005). folded gastrulation, cell shape change and the control of myosin localization. Development *132*, 4165–4178.

Dearolf, C. R., Hersperger, E., and Shearn, A. (1988). Developmental consequences of awdb3, a cell-autonomous lethal mutation of Drosophila induced by hybrid dysgenesis. Dev. Biol. *129*, 159–168.

Edwards, K. A., and Kiehart, D. P. (1996). Drosophila nonmuscle myosin II has multiple essential roles in imaginal disc and egg chamber morphogenesis. Development *122*, 1499–1511.

Escudero, L. M., Bischoff, M., and Freeman, M. (2007). Myosin II regulates complex cellular arrangement and epithelial architecture in Drosophila. Dev. Cell *13*, 717–729.

Fristrom, D. (1988). The cellular basis of epithelial morphogenesis. A review. Tissue Cell *20*, 645–690.

Fristrom, D., and Fristrom, J. W. (1975). The mechanism of evagination of imaginal discs of *Drosophila melanogaster*. 1. General considerations. Dev. Biol. *43*, 1–23.

Fukata, Y., Kimura, K., Oshiro, N., Saya, H., Matsuura, Y., and Kaibuchi, K. (1998). Association of the myosin-binding subunit of myosin phosphatase and moesin: dual regulation of moesin phosphorylation by Rho-associated kinase and myosin phosphatase. J. Cell Biol. *141*, 409–418.

Gallagher, P. J., Herring, B. P., Griffin, S. A., and Stull, J. T. (1991). Molecular characterization of a mammalian smooth muscle myosin light chain kinase. J. Biol. Chem. *266*, 23936–23944.

Gally, C., Wissler, F., Zahreddine, H., Quintin, S., Landmann, F., and Labouesse, M. (2009). Myosin II regulation during *C. elegans* embryonic elongation: LET-502/ROCK, MRCK-1 and PAK-1, three kinases with different roles. Development *136*, 3109–3119.

Gong, W. J., and Golic, K. G. (2003). Ends-out, or replacement, gene targeting in Drosophila. Proc. Natl. Acad. Sci. USA. *100*, 2556–2561.

Gotwals, P. J., and Fristrom, J. W. (1991). Three neighboring genes interact with the Broad-Complex and the Stubble-stubbloid locus to affect imaginal disc morphogenesis in Drosophila. Genetics *127*, 747–759.

Grusche, F. A., Hidalgo, C., Fletcher, G., Sung, H.-H., Sahai, E., and Thompson, B. J. (2009). Sds22, a PP1 phosphatase regulatory subunit, regulates epithelial cell polarity and shape. BMC Dev. Bio. *9*, 14.

Hagerty, L., Weitzel, D. H., Chambers, J., Fortner, C. N., Brush, M. H., Loiselle, D., Hosoya, H., and Haystead, T. A. (2007). ROCK1 phosphorylates and activates zipper-interacting protein kinase. J. Biol. Chem. *282*, 4884–4893.

Halsell, S. R., Chu, B. I., and Kiehart, D. P. (2000). Genetic analysis demonstrates a direct link between rho signaling and nonmuscle myosin function during drosophila morphogenesis. Genetics *156*, 469.

Hipfner, D. R., Keller, N., and Cohen, S. M. (2004). Slik Sterile-20 kinase regulates Moesin activity to promote epithelial integrity during tissue growth. Genes Dev. *18*, 2243–2248.

Inbal, B., Shani, G., Cohen, O., Kissil, J. L., and Kimchi, A. (2000). Death-associated protein kinase-related protein 1, a novel serine/threonine kinase involved in apoptosis. Mol. Cell. Biol. *20*, 1044–1054.

Ito, M., Nakano, T., Erdodi, F., and Hartshorne, D. J. (2004). Myosin phosphatase: structure, regulation and function. Mol. Cell Biochem. *259*, 197–209.

Jordan, P., and Karess, R. (1997). Myosin light chain-activating phosphorylation sites are required for oogenesis in Drosophila. J. Cell Biol. *139*, 1805–1819.

Katoh, K., Kano, Y., Amano, M., Kaibuchi, K., and Fujiwara, K. (2001). Stress fiber organization regulated by MLCK and Rho-kinase in cultured human fibroblasts. Am. J. Physiol. Cell Physiol. *280*, C1669–C1679.

Kawai, T., Nomura, F., Hoshino, K., Copeland, N. G., Gilbert, D. J., Jenkins, N. A., and Akira, S. (1999). Death-associated protein kinase 2 is a new calcium/calmodulin-dependent protein kinase that signals apoptosis through its catalytic activity. Oncogene *18*, 3471–3480.

Kawano, Y., Fukata, Y., Oshiro, N., Amano, M., Nakamura, T., Ito, M., Matsumura, F., Inagaki, M., and Kaibuchi, K. (1999). Phosphorylation of myosin-binding subunit (MBS) of myosin phosphatase by Rho-kinase in vivo. J. Cell Biol. *147*, 1023–1038.

Kimura, K., Ito, M., Amano, M., Chihara, K., Fukata, Y., Nakafuku, M., Yamamori, B., Feng, J., Nakano, T., Okawa, K., Iwamatsu, A., and Kaibuchi, K. (1996). Regulation of myosin phosphatase by Rho and Rho-associated kinase (Rho-kinase). Science *273*, 245–248.

Kogel, D., Plottner, O., Landsberg, G., Christian, S., and Scheidtmann, K. H. (1998). Cloning and characterization of Dlk, a novel serine/threonine kinase that is tightly associated with chromatin and phosphorylates core histones. Oncogene *17*, 2645–2654.

Kuo, J. C., Lin, J. R., Staddon, J. M., Hosoya, H., and Chen, R. H. (2003). Uncoordinated regulation of stress fibers and focal adhesions by DAP kinase. J. Cell Sci. *116*, 4777–4790.

Kureishi, Y., Kobayashi, S., Amano, M., Kimura, K., Kanaide, H., Nakano, T., Kaibuchi, K., and Ito, M. (1997). Rho-associated kinase directly induces smooth muscle contraction through myosin light chain phosphorylation. J. Biol. Chem. *272*, 12257–12260.

Lecuit, T., and Lenne, P. F. (2007). Cell surface mechanics and the control of cell shape, tissue patterns and morphogenesis. Nat. Rev. Mol. Cell Biol. *8*, 633–644.

Lee, A., and Treisman, J. E. (2004). Excessive Myosin activity in mbs mutants causes photoreceptor movement out of the Drosophila eye disc epithelium. Mol. Biol. Cell *15*, 3285–3295.

Manning, G., Whyte, D. B., Martinez, R., Hunter, T., and Sudarsanam, S. (2002). The protein kinase complement of the human genome. Science *298*, 1912–1934.

Mao, J., Qiao, X., Luo, H., and Wu, J. (2006). Transgenic drak2 overexpression in mice leads to increased T cell apoptosis and compromised memory T cell development. J. Biol. Chem. *281*, 12587–12595.

McGargill, M. A., Wen, B. G., Walsh, C. M., and Hedrick, S. M. (2004). A deficiency in Drak2 results in a T cell hypersensitivity and an unexpected resistance to autoimmunity. Immunity *21*, 781–791.

Mitonaka, T., Muramatsu, Y., Sugiyama, S., Mizuno, T., and Nishida, Y. (2007). Essential roles of myosin phosphatase in the maintenance of epithelial cell integrity of Drosophila imaginal disc cells. Dev. Biol. *309*, 78–86.

Mizuno, T., Amano, M., Kaibuchi, K., and Nishida, Y. (1999). Identification and characterization of Drosophila homolog of Rho-kinase. Gene *238*, 437–444.

Mizuno, T., Tsutsui, K., and Nishida, Y. (2002). Drosophila myosin phosphatase and its role in dorsal closure. Development *129*, 1215–1223.

Murata-Hori, M., Fukuta, Y., Ueda, K., Iwasaki, T., and Hosoya, H. (2001). HeLa ZIP kinase induces diphosphorylation of myosin II regulatory light chain and reorganization of actin filaments in nonmuscle cells. Oncogene *20*, 8175–8183.

Murata-Hori, M., Suizu, F., Iwasaki, T., Kikuchi, A., and Hosoya, H. (1999). ZIP kinase identified as a novel myosin regulatory light chain kinase in HeLa cells. FEBS Lett. *451*, 81–84.

Parks, A. L., *et al*. (2004). Systematic generation of high-resolution deletion coverage of the *Drosophila melanogaster* genome. Nat. Genet. *36*, 288–292.

Pelled, D., Raveh, T., Riebeling, C., Fridkin, M., Berissi, H., Futerman, A. H., and Kimchi, A. (2002). Death-associated protein (DAP) kinase plays a central role in ceramide-induced apoptosis in cultured hippocampal neurons. J. Biol. Chem. *277*, 1957–1961.

Perez-Perez, J. M., Candela, H., and Micol, J. L. (2009). Understanding synergy in genetic interactions. Trends Genet. *25*, 368–376.

Quintin, S., Gally, C., and Labouesse, M. (2008). Epithelial morphogenesis in embryos: asymmetries, motors and brakes. Trends Genet. *24*, 221–230.

Raveh, T., Droguett, G., Horwitz, M. S., DePinho, R. A., and Kimchi, A. (2001). DAP kinase activates a p19ARF/p53-mediated apoptotic checkpoint to suppress oncogenic transformation. Nat. Cell Biol. *3*, 1–7.

Sanjo, H., Kawai, T., and Akira, S. (1998). DRAKs, novel serine/threonine kinases related to death-associated protein kinase that trigger apoptosis. J. Biol. Chem. *273*, 29066–29071.

Sellers, J. R. (1985). Mechanism of the phosphorylation-dependent regulation of smooth muscle heavy meromyosin. J. Biol. Chem. *260*, 15815–15819.

Speck, O., Hughes, S. C., Noren, N. K., Kulikauskas, R. M., and Fehon, R. G. (2003). Moesin functions antagonistically to the Rho pathway to maintain epithelial integrity. Nature *421*, 83–87.

Thibault, S. T., *et al*. (2004). A complementary transposon tool kit for *Drosophila melanogaster* using P and piggyBac. Nat. Genet. *36*, 283–287.

Tong, A., Lynn, G., Ngo, V., Wong, D., Moseley, S. L., Ewbank, J. J., Goncharov, A., Wu, Y. C., Pujol, N., and Chisholm, A. D. (2009). Negative regulation of *Caenorhabditis elegans* epidermal damage responses by death-associated protein kinase. Proc. Natl. Acad. Sci. USA. *106*, 1457–1461.

Totsukawa, G., Yamakita, Y., Yamashiro, S., Hartshorne, D. J., Sasaki, Y., and Matsumura, F. (2000). Distinct roles of ROCK (Rho-kinase) and MLCK in spatial regulation of MLC phosphorylation for assembly of stress fibers and focal adhesions in 3T3 fibroblasts. J. Cell Biol. *150*, 797–806.

Ueda, K., Murata-Hori, M., Tatsuka, M., and Hosoya, H. (2002). Rho-kinase contributes to diphosphorylation of myosin II regulatory light chain in nonmuscle cells. Oncogene *21*, 5852–5860.

VanHook, A., and Letsou, A. (2008). Head involution in Drosophila: genetic and morphogenetic connections to dorsal closure. Dev. Dyn. *237*, 28–38.

Vereshchagina, N., Bennett, D., Szoor, B., Kirchner, J., Gross, S., Vissi, E., White-Cooper, H., and Alphey, L. (2004). The essential role of PP1beta in Drosophila is to regulate nonmuscle myosin. Mol. Biol. Cell *15*, 4395–4405.

Vicente-Manzanares, M., Ma, X., Adelstein, R. S., and Horwitz, A. R. (2009). Non-muscle myosin II takes centre stage in cell adhesion and migration. Nat. Rev. Mol. Cell Biol. *10*, 778–790.

Winter, C. G., Wang, B., Ballew, A., Royou, A., Karess, R., Axelrod, J. D., and Luo, L. (2001). Drosophila Rho-associated kinase (Drok) links Frizzled-mediated planar cell polarity signaling to the actin cytoskeleton. Cell *105*, 81–91.